Materials & Design 131 (2017) 167–176

Contents lists available at ScienceDirect

Materials & Design

journal homepage: www.elsevier.com/locate/matdes

Effect of primary recrystallization microstructure on abnormal growth of Goss grains in a twin-roll cast grain-oriented electrical steel

Hong-Yu Song[a], Hai-Tao Liu[a,*], John J. Jonas[b], Guo-Dong Wang[a]

[a] State Key Laboratory of Rolling and Automation, Northeastern University, Shenyang 110819, PR China
[b] Materials Engineering Department, McGill University, 3610 University Street, Montreal H3A 0C5, Canada

ARTICLE INFO

Keywords:
Goss grains
Twin-roll casting
Grain-oriented electrical steel
Cold rolling
Abnormal grain growth

ABSTRACT

Various primary recrystallization microstructures and textures were produced in a twin-roll cast grain-oriented electrical steel by employing different routes. The relationship between the primary recrystallization microstructure and texture and the abnormal growth of secondary Goss grains was investigated. The results show that the cold rolling reductions have a significant influence on secondary recrystallization by changing the primary recrystallization microstructure. Sheet processed by single-stage cold rolling with 88.3% reduction displayed the poorest secondary recrystallization microstructure as it contained many small equiaxed grains. By contrast, the employment of two-stage cold rolling markedly improved the secondary recrystallization microstructure. In the case of two moderate reductions of 65.2% and 66.3%, dense deformation substructures formed during both the first and second cold rolling, leading to a homogeneous primary recrystallization microstructure together with a strong γ-fiber texture. In this way, a suitable secondary recrystallization microstructure consisting of large Goss grains was produced. In the case of the inappropriate reductions, many large λ- and α-grains in the primary recrystallization matrix blocked the growth of secondary Goss grains along the transverse direction, resulting in a poor secondary recrystallization microstructure.

1. Introduction

Twin-roll casting is a novel 'near-net-shape' forming process by means of which thin strips can be produced directly from the melt [1,2]. Recent progress in twin-roll casting has made it possible to produce grain-oriented electrical steels using this technique [3–5]. For example, Liu et al. [3] and Song et al. [4,5] have shown that 0.23–0.27 mm thick grain-oriented electrical steel sheets can be successfully fabricated using twin-roll casting. In conventional processing, the {110} ⟨001⟩ Goss texture is introduced near the surface during hot rolling as a result of the intense shear associated with roll friction [6,7]. This component survives through subsequent processing and provides the Goss nuclei necessary for successful secondary recrystallization [8,9]. The importance of the surface layer of the hot rolled sheet was demonstrated in experiments in which the Goss-containing layer was removed, resulting in incomplete secondary recrystallization [10]. Thus, hot rolling is generally considered to be indispensible during the conventional processing of grain-oriented electrical steel.

More recently, Song et al. [11] and Fang et al. [12] have shown that grain-oriented electrical steel sheet can be successfully produced without hot rolling by employing a particular twin-roll casting route. According to this method, the origin and development of the Goss orientation differs from those in the conventional process. In the conventional process, the effects of primary recrystallization on the secondary recrystallization behavior have been investigated in detail. Various models have been developed to explain the selective growth of the Goss grains, i.e. the size advantage model [13,14], the coincidence site lattice (CSL) model [15–17], the high energy (HE) model [18–20] and the solid-state wetting model [21–23]. When the twin-roll casting route is employed, the microstructures and textures produced by primary recrystallization differ considerably from those resulting from the conventional process. In the latter, the Goss texture is the major component of the primary recrystallization texture when the two-stage route is employed. By contrast, in the strip casting process, a strong γ-fiber and a weak Goss component are produced, leading to distinct secondary recrystallization behaviors. The relation between the characteristics of the primary recrystallization microstructure and the abnormal growth of secondary Goss grains is still not clearly understood.

In the present paper, various primary recrystallization microstructures and textures were produced in a twin-roll cast grain-oriented electrical steel by employing different processing routes. The interaction between the primary recrystallization behavior and the abnormal

* Corresponding author.
E-mail address: liuht@ral.neu.edu.cn (H.-T. Liu).

http://dx.doi.org/10.1016/j.matdes.2017.06.016
Received 10 January 2017; Received in revised form 6 June 2017; Accepted 6 June 2017
Available online 07 June 2017
0264-1275/

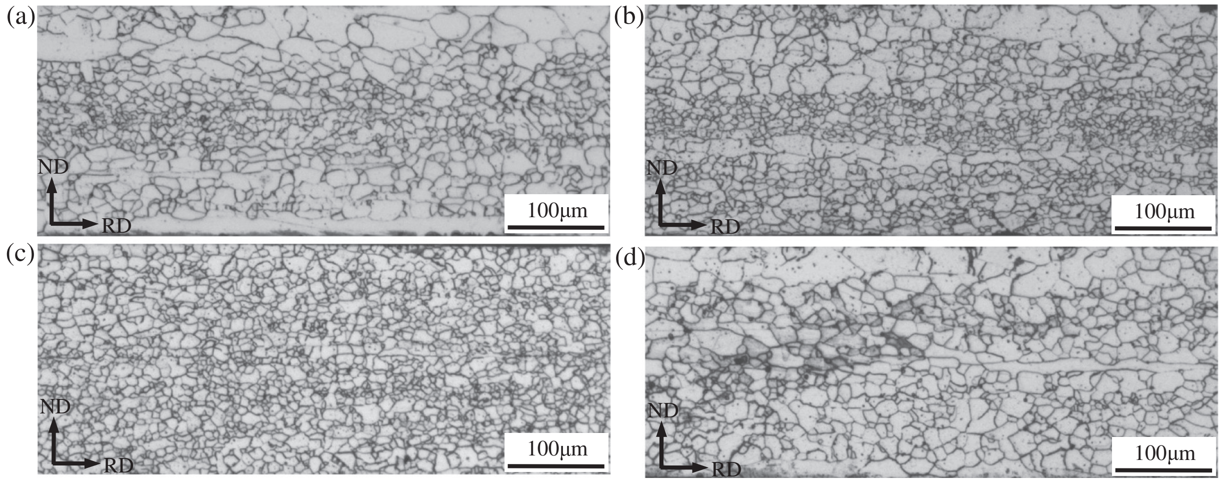

Fig. 1. Microstructures of the (a) RI-PRA, (b) RII-PRA, (c) RIII-PRA and (d) RIV-PRA sheets.

growth of secondary Goss grains was investigated. This work has led to an increased understanding of the development of sharp Goss textures in twin-roll cast grain-oriented electrical steels, as will be seen below.

2. Experimental procedures

The chemical composition (wt%) of the tested steel was 3.32 Si, 0.0026 C, 0.064 Mn, 0.024 S, 0.035 Al, 0.0093 N and balance Fe. A 2.3 mm-thick as-cast strip was produced using a vertical type twin-roll caster. During casting, a relatively high melt superheat was employed so as to produce a coarse solidification microstructure composed of large columnar grains. The experimental details of this process have been reported previously [24,25]. The as-cast strips were annealed at 950 °C for 4 min and water quenched. Here, four different routes were employed to produce the cold rolled sheets: (RI) the annealed sheets were directly cold rolled to the final thickness of 0.27 mm using a reduction of 88.3%; (RII) the annealed sheets were first subjected to a cold rolling using a reduction of 56.5%, intermediate annealed at 830 °C for 3 min, and then cold rolled to 0.27 mm using a reduction of 73.0%; (RIII) the annealed sheets were first cold rolled to 0.8 mm using a reduction of 65.2%, intermediate annealed at 830 °C for 3 min, and then cold rolled to 0.27 mm using a reduction of 66.3%; (RIV) the annealed sheets were first cold rolled down to 0.6 mm using a reduction of 73.9%, intermediate annealed at 830 °C for 3 min, and cold rolled to a final thickness of 0.27 mm using a reduction of 55.0%. In all four cases, primary recrystallization annealing was carried out at 830 °C for 3 min. Finally, the sheets were heated up to 1200 °C at a heating rate of 20 °C/h and held at 1200 °C for 10 h. For convenience, the samples are denoted here as first cold rolled (FCR) sheet, primary recrystallization annealed (PRA) sheet and secondary recrystallization annealed (SRA) sheet.

The primary recrystallization microstructures were etched with 4% nital and examined using a Leica optical microscope. The secondary recrystallization microstructures were revealed by etching suitably ground samples with 10% hydrochloric acid. For characterization of the texture, the orientation distribution functions (ODFs) were calculated from three incomplete {110}, {200} and {211} pole figures by the series expansion method ($l_{max} = 22$) developed by Bunge [26,27]. For the electron backscatter diffraction (EBSD) measurements, the samples were wet ground using silicon carbide papers, mechanically polished and electropolished with a 14% perchloric acid/alcohol solution. The EBSD system was installed on a Zeiss Ultra 55 scanning electron microscope (SEM). The size distribution of the inhibitors was determined using SEM. The chemical composition of the inhibitors was verified by means of energy dispersive X-ray spectroscopy.

3. Results

3.1. Microstructure and texture of the as-cast strip

The microstructure of the as-cast strip was composed of large columnar ferrite grains, as reported previously [11]. The associated texture consisted of the λ-fiber texture (〈001〉//ND) and did not vary significantly through the thickness [11]. These characteristics have been attributed to the high melt superheat [28]. It is important to note that the as-cast strip was not subjected to any deformation before annealing. Thus, the as-cast microstructure and texture were not changed because the as-cast strip did not undergo any recrystallization or phase transformation.

3.2. Primary recrystallization microstructure and texture

The microstructures and textures of the primary recrystallization annealed sheets subjected to the four different routes are shown in Figs. 1 and 2, respectively. As can be seen, the RIII-PRA sheet had the most uniform microstructure consisting entirely of equiaxed ferrite grains with a size range of 10–23 μm, Fig. 1c. The texture was characterized by a strong γ-fiber texture, a medium α-fiber texture, and a weak Goss component. It is of particular note that many Goss grains were distributed throughout the thickness (Fig. 3b) and that these were characterized by grain boundaries of intermediate misorientations (20–45°). By contrast, the boundaries of the matrix as a whole had fewer misorientations in this range (Fig. 4a), in consistency with earlier observations [18–20,29]. Such boundaries have higher energies and thus facilitate coarsening of the inhibitors as well as the reduction of their pinning effects, leading to the selective growth of the Goss grains. This kind of grain boundary characteristic distribution (GBCD) is considered to facilitate the abnormal growth of Goss grains during secondary recrystallization annealing [18–20].

By contrast, the PRA sheets produced by the three other routes exhibited similar inhomogeneous microstructures with large elongated grains at the surface and relatively fine grains in the center, Fig. 1a, b and d. On the RD-TD section, the large elongated grains can be seen to be distributed inhomogeneously and separated by fine grained regions. The RI-PRA sheet exhibited a strong α-fiber texture at the surface, a strong {111}〈112〉 component and a medium λ-fiber texture through the thickness. The texture of the RII-PRA sheet was characterized by a strong partial α-fiber running from {001}〈110〉 to {111}〈110〉, a distinct λ-fiber and a weak γ-fiber from the surface to the 1/4 layer, these were associated with a medium α-fiber and a {111}〈112〉 component in the center. It is of interest that the RIV-PRA sheet displays a texture that is similar to that of the RII-PRA sheet. One difference is